Journal of Nuclear Materials 493 (2017) 294–302

Contents lists available at ScienceDirect

Journal of Nuclear Materials

journal homepage: www.elsevier.com/locate/jnucmat

Stress intensification at grain boundary free ends in anisotropic materials - Application to austenitic stainless steel Intergranular Stress Corrosion Cracking susceptibility

G. Meric de Bellefon [a, *], J.C. van Duysen [b, c, d]

[a] University of Wisconsin-Madison, United States
[b] University of Tennessee-Knoxville, United States
[c] Unité Matériaux et Transformation (UMET) CNRS, Université de Lille, France
[d] Ecole Nationale Supérieure de Chimie de Lille, France

ARTICLE INFO

Article history:
Received 23 February 2017
Received in revised form
30 April 2017
Accepted 21 May 2017
Available online 23 May 2017

ABSTRACT

Most studies on Intergranular Stress Corrosion Cracking (IGSCC) in Light Water Reactor environment consider the macroscopic applied stress as the relevant mechanical parameter to characterize crack initiation. Progress in understanding, modeling, and forecasting IGSCC could be made by correlating crack initiation susceptibility to the stress field at crack initiation sites. Through finite element method (FEM) calculations, the present article assesses this stress field in polycrystalline 316 stainless steel and identifies key parameters controlling local stress intensification. It is in particular shown that the auxetic behavior (i.e., negative Poisson's ratio) of 316 single crystals in some orientations plays an important role. FEM calculation results are used to set up a preliminary expression that can be used to rank IGSCC initiation sensitivity of components made of the same fcc alloy (i.e., austenitic stainless steels, Ni-based alloys) from their surface texture. Further work is in progress to integrate influence of grain boundary triple junctions and validate the whole approach against experimental SCC data.

1. Introduction

Intergranular Stress Corrosion Cracking (IGSCC) is a recurring issue in Light Water Reactors (LWR). Since the early 1960s (e.g. [1]), IGSCC was successively reported on: sensitized 304 and 316 austenitic stainless steels in Boiling Water Reactors (BWR), nickel-based alloys (alloys 600 then X750) in primary or secondary water of Pressurized Water Reactors (PWR), irradiated stainless steels as well as cold-worked non-sensitized stainless steels in PWR and BWR. Such degradation entailed large maintenance costs, e.g., to replace steam generators, reactor vessel heads, or baffle plate bolts in PWR.

Many research programs have been carried out worldwide [2] to find out solutions to mitigate or suppress IGSCC in LWR. Through corrosion tests, those programs mostly aimed to understand and quantify the role of stress, water chemistry, electrochemical potential, irradiation, creep, hydrogen charging, material deformation history, and surface machining (e.g. [3–11]). Experimental studies were also carried out to characterize phases, chemistry, crack morphology, and plasticity at crack tips (e.g. [12–14]). This experimental endeavor uncovered some of the key parameters contributing to SCC (e.g. [15]) and enabled the development of predictive models (e.g., see review for cold-worked austenitic stainless steels in Ref. [16]). It also supports the current effort on multi-scale modeling of SCC (e.g. [17]). This outcome was highly useful to select materials and operational conditions that help to limit IGSCC degradation in LWR. However, it must be admitted that a full understanding of the mechanisms controlling this degradation has not been established yet, and further work is still needed.

It is well known that SCC phenomena require a proper combination of stress, environment, and material conditions. They are in general described in two main stages: crack initiation and crack propagation. From a mechanical standpoint, crack propagation rate is in general correlated with the stress field at crack tip. This stress field is evaluated through classical approaches used in Fracture Mechanics (e.g. [18]) and captures local intensification of the

* Corresponding author. Engineering Physics, University of Wisconsin-Madison, 1500 Engineering Drive, Madison, WI 53706, United States.
E-mail address: mericdebelle@wisc.edu (G. Meric de Bellefon).

http://dx.doi.org/10.1016/j.jnucmat.2017.05.028
0022-3115/

macroscopic applied stress. For the initiation stage, most modeling studies and analysis of experimental data consider the macroscopic applied stress as the relevant mechanical parameter [19].

Under static loading and LWR conditions, SCC initiation sites for austenitic stainless steels and nickel-based alloys are the emergences of grain boundaries on the free surface. These emergences will be named grain boundary free-ends in the rest of this document. Owing to anisotropy of *fcc* single crystals (see Appendix), grain boundaries in *fcc* alloys have to be considered as interfaces between materials with different elastic responses when stressed. The stress field at such interfaces has been the subject of many studies, in particular in the area of adhesive joints for structural applications. As shown in Fig. 1, under a tensile stress in air at room temperature, it is experimentally observed (e.g. [20]) that the onset of fracture on these joints mainly happens at the emergences of the interfaces between the involved materials (e.g., a metal and an adhesive such as epoxy) on the specimen surface (interface free-ends). This preferential location is attributed to a local stress intensification resulting from both the presence of the free surfaces and the elastic mismatch between the materials [25]. A stress intensification can also been expected at grain boundary free-ends in austenitic stainless steels and nickel-based alloys, while being not high enough to initiate a crack without a proper combination of environment and other material conditions (for such alloys, SCC-type tests carried out in inert atmosphere do not lead to any crack). Several models have been developed to evaluate the stress intensification at interfaces between isotropic or anisotropic materials with different elastic properties (e.g., [21–27]. For isotropic materials [25,28,29], the maximum stress appears to be located several degrees away from the interface in the stiffer material.

Several finite element method (FEM) studies confirmed that the applied stress might be intensified at grain boundary free-ends in austenitic stainless steels and nickel-based alloys [30,31]. Progress in understanding, modeling, and forecasting IGSCC in LWR could be made by identifying the key parameters controlling this stress intensification, and correlating crack initiation times and sites with those parameters. This should also help to reduce SCC susceptibility of components by optimizing their manufacturing process or the chemical composition of their alloy (chemical composition impacts the texture thus the nature of grain boundaries). The present work relies on FEM calculations to i) assess stress intensification at grain boundary free-ends in 316 stainless steel under constant elastic loading, and ii) identify the key parameters controlling this stress intensification. It is part of a broader effort to tailor austenitic stainless steels to LWR applications [32].

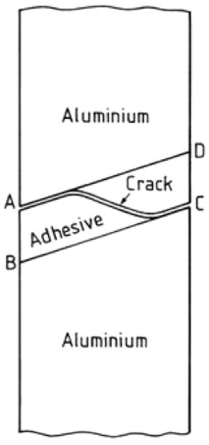

Fig. 1. Fracture at the interfaces between two materials with different elastic properties. Cracks start at interface free-ends A and C, grow along the interface and deflect into the adhesive [20].

2. Methods

2.1. FEM model

We consider two 316 grains (Grain 1 and Grain 2) at the surface of a tensile specimen under a constant macroscopic applied stress σ. The specimen is solicited in its elastic domain (i.e., σ is lower than the flow stress). This latter condition fulfills conventional structural design rules, which in general limit in-service mechanical loading to 60% of yield stress (80% for severe loading). The grains are anisotropic, which implies that their elastic behavior depends on their orientation with respect to the tensile direction. The calculation of the anisotropic elastic constants is detailed in the Appendix. The presence of an oxide layer on the specimen surface is not taken into account.

2.2. FEM calculations

The stress field near grain boundary free-ends was determined through linear elastic FEM calculations run with the commercial LISA program. The simulated model specimen is shown in Fig. 2, along with the considered laboratory basis (e_1, e_2, e_3). It has two anisotropic 316 grains (Grain 1 and Grain 2) embedded in an isotropic 316 matrix. The grain boundary between the two grains is perpendicular to the applied stress, based on results of [30] that showed that this configuration leads to the highest stress intensification. As mentioned in section 5, other orientations are currently under study. The grain boundary is limited to a line, which is a purely theoretical case since real grain boundaries have a non-zero thickness. Thickness, width, and height of the model specimen are 40, 300, and 300 μm, respectively. The height of both grains is 37.5 μm. Boundary conditions are the following (see Fig. 2a):

- displacement along e_2 is null on face D,
- macroscopic stress is applied on face D'.
- in order to simulate the behavior of two grains embedded in a test specimen and having only one free surface, displacement is null along e_3 on surfaces B and B' (i.e., plane strain conditions), and null along e_1 on face A'.

With those constraints, the model specimen behaves as if it was inserted into a larger test specimen stressed along e_2 and having a free surface comprising face A. The meshes are parallelepiped-shaped elements that get smaller closer to the grain boundary (see Fig. 2b).

As the effect of temperature on the elastic constants of stainless steels is poorly known, the calculations were run at room temperature (RT). As discussed in section 4, the obtained results are expected to be meaningful in the LWR in-service temperature range (≈280–370 °C). Several teams have experimentally measured the RT elastic properties of annealed Fe-Cr-Ni alloy single crystals (see review in Ref. [33]). We used stiffness values proposed in Ref. [34] for 316 single crystals: $c_{11} = 2.06\ 10^{11}$ N/m^2, $c_{12} = 1.33\ 10^{11}$ N/m^2 and $c_{44} = 1.19\ 10^{11}$ N/m^2. We note E_i the Young's modulus along direction i, G_{ij} the shear modulus along j in plan i (ratio of the shear stress to the shear strain along direction j in the plan perpendicular to i, $G_{ij} = G_{ji}$), and ν_{ij} the Poisson's ratio along j for a stretching along i (ratio of length evolution along direction j to that along the stretching direction i, ν_{ij} may differ from ν_{ji}). For the isotropic 316 matrix, we used the values proposed in Ref. [35]: $E = 1.95\ 10^{11}$ N/m^2 and $\nu = 0.29$.

Calculations were run with an applied stress of 300 MPa, which is a meaningful value considering the possible range of RT flow